Spectrochimica Acta Part A: Molecular and Biomolecular Spectroscopy 123 (2014) 416–420

Contents lists available at ScienceDirect

Spectrochimica Acta Part A: Molecular and Biomolecular Spectroscopy

journal homepage: www.elsevier.com/locate/saa

Raman spectroscopy of the arsenate minerals maxwellite and in comparison with tilasite

Ray L. Frost [a,*], Ricardo Scholz [b], Andrés López [a], Yunfei Xi [a]

[a] School of Chemistry, Physics and Mechanical Engineering, Science and Engineering Faculty, Queensland University of Technology, GPO Box 2434, Brisbane Queensland 4001, Australia

[b] Geology Department, School of Mines, Federal University of Ouro Preto, Campus Morro do Cruzeiro, Ouro Preto, MG 35,400-00, Brazil

HIGHLIGHTS

- We have studied the arsenate mineral maxwellite $NaFe^{3+}(AsO_4)F$.
- A comparison is made with tilasite $CaMg(AsO_4)F$.
- Chemical analysis shows that maxwellite is composed of Fe, Na and Ca with minor amounts of Mn and Al.
- Raman and infrared bands are assigned.
- The molecular structure of maxwellite is assessed.

GRAPHICAL ABSTRACT

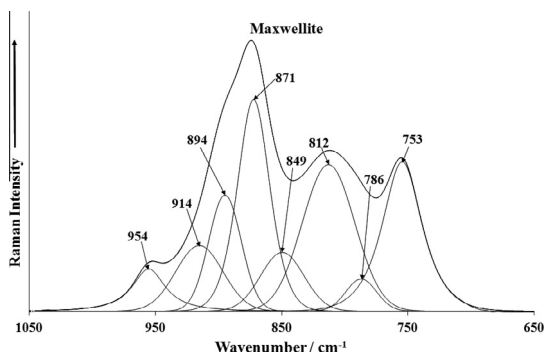

ARTICLE INFO

Article history:
Received 24 September 2013
Received in revised form 2 December 2013
Accepted 11 December 2013
Available online 25 December 2013

Keywords:
Raman spectroscopy
Maxwellite
Tilasite
Durangite
Arsenate

ABSTRACT

Maxwellite $NaFe^{3+}(AsO_4)F$ is an arsenate mineral containing fluoride and forms a continuous series with tilasite $CaMg(AsO_4)F$. Both maxwellite and tilasite form a continuous series with durangite $NaAl^{3+}(AsO_4)$-F. We have used the combination of scanning electron microscopy with EDS and vibrational spectroscopy to chemically analyse the mineral maxwellite and make an assessment of the molecular structure. Chemical analysis shows that maxwellite is composed of Fe, Na and Ca with minor amounts of Mn and Al. Raman bands for tilasite at 851 and 831 cm^{-1} are assigned to the Raman active ν_1 symmetric stretching vibration (A_1) and the Raman active triply degenerate ν_3 antisymmetric stretching vibration (F_2). The Raman band of maxwellite at 871 cm^{-1} is assigned to the ν_1 symmetric stretching vibration and the Raman band at 812 cm^{-1} is assigned to the ν_3 antisymmetric stretching vibration. The intense Raman band of tilasite at 467 cm^{-1} is assigned to the Raman active triply degenerate ν_4 bending vibration (F_2). Raman band at 331 cm^{-1} for tilasite is assigned to the Raman active doubly degenerate ν_2 symmetric bending vibration (E). Both Raman and infrared spectroscopy do not identify any bands in the hydroxyl stretching region as is expected.

Introduction

Maxwellite $NaFe^{3+}(AsO_4)F$ [1] is an arsenate mineral containing fluoride and forms a continuous series with tilasite $CaMg(AsO_4)F$ [2,3]. Both minerals may form a continuous series with durangite [4–6]. These three minerals all form part of the tilasite mineral group which are anhydrous arsenates with an additional anion [7]. In the case of these three minerals, it is the fluoride anion. Maxwellite is bright red whereas the colour of tilasite varies according to the mineral composition from violet gray, green, gray, to pink brown. Durangite colour is light to dark orange–red, red; green; orange–yellow in artificial light. The colour of the solid solutions of these three minerals will be dependent on the composition

* Corresponding author. Tel.: +61 7 3138 2407; fax: +61 7 3138 1804.
E-mail address: r.frost@qut.edu.au (R.L. Frost).

1386-1425/$ - see front matter © 2013 Elsevier B.V. All rights reserved.
http://dx.doi.org/10.1016/j.saa.2013.12.081

of the mineral. Maxwellite is named after Charles Henry Maxwell of U.S. Geological Survey. Tilasite is named after Daniel Tilas (1712-1772), a Swedish mining engineer. The type mineral specimen of durangite originates from the Barranca tin mine, about 30 km northeast of Coneto de Comonfort, Durango, Mexico and thus durangite is named after its place of origin.

All three minerals are monoclinic [1,8,9]. Maxwellite cell parameters [8] are $a = 7.161$ Å, $b = 8.78$ Å, $c = 6.687$ Å, $Z = 4$; beta = 114.58° $V = 382.34$ Den(Calc) = 4.11 and the values may be compared with tilasite whose cell parameters are $a = 7.553$ Å, $b = 8.951$ Å, $c = 6.701$ Å, $Z = 4$; beta = 120.967° $V = 388.46$ [10]. The values for durangite are $a = 6.579$ Å, $b = 8.523$ Å, $c = 7.048$ Å, $Z = 4$; beta = 115.47° $V = 356.79$ [11,12]. The cell parameters of all three minerals are very close. It is likely that these cell parameters are a function of the cation content. Crystals of maxwellite are prismatic with crystals shaped like slender prisms such as with tourmaline and form aggregates of numerous individual crystals or clusters. The habit of tilasite is quite similar but forms uniformly indistinguishable crystals forming large masses.

Raman spectroscopy has proven very useful for the study of minerals. Indeed Raman spectroscopy has proven most useful for the study of diagenetically related minerals as often occurs with minerals containing sulphate, arsenate and/or phosphate groups. Raman spectroscopy is especially useful when the minerals are X-ray non-diffracting or poorly diffracting and very useful for the study of amorphous and colloidal minerals. This paper is a part of systematic studies of vibrational spectra of minerals of secondary origin in the oxide supergene zone. In this work, we attribute bands at various wavenumbers to vibrational modes of maxwellite and tilasite using Raman spectroscopy and relate the spectra to the structure of the mineral.

Experimental

Minerals

The minerals were incorporated into the collection of the Geology Department of the Federal University of Ouro Preto, Minas Gerais, Brazil, with sample codes SAC-119 (maxwellite) and SAC-117 (tilasite). The samples were gently crushed and the associated minerals were removed under a stereomicroscope Leica MZ4. Scanning electron microscopy (SEM) was applied to support the chemical characterisation. Details of the mineral have been published (page 344 (maxwellite) and p589 (tilasite), vol. IV) [13].

Raman spectroscopy

Crystals of maxwellite or tilasite were placed on a polished metal surface on the stage of an Olympus BHSM microscope, which is equipped with 10×, 20×, and 50× objectives. The microscope is part of a Renishaw 1000 Raman microscope system, which also includes a monochromator, a filter system and a CCD detector (1024 pixels). The Raman spectra were excited by a Spectra-Physics model 127 He–Ne laser producing highly polarised light at 633 nm and collected at a nominal resolution of 2 cm^{-1} and a precision of ±1 cm^{-1} in the range between 100 and 4000 cm^{-1}. Repeated acquisition on the crystals using the highest magnification (50×) was accumulated to improve the signal to noise ratio in the spectra. Spectra were calibrated using the 520.5 cm^{-1} line of a silicon wafer.

Infrared spectroscopy

Infrared spectra were obtained using a Nicolet Nexus 870 FTIR spectrometer with a smart endurance single bounce diamond ATR cell. Spectra over the 4000–525 cm^{-1} range were obtained by the co-addition of 128 scans with a resolution of 4 cm^{-1} and a mirror velocity of 0.6329 cm/s. Spectra were co-added to improve the signal to noise ratio.

Band component analysis was undertaken using the Jandel 'Peakfit' (Erkrath, Germany) software package which enabled the type of fitting function to be selected and allowed specific parameters to be fixed or varied accordingly. Band fitting was done using a Lorentz–Gauss cross-product function with the minimum number of component bands used for the fitting process. The Lorentz–Gauss ratio was maintained at values greater than 0.7 and fitting was undertaken until reproducible results were obtained with squared correlations (r^2) greater than 0.995. Band fitting of the spectra is quite reliable providing there is some band separation or changes in the spectral profile.

Results and discussion

Chemistry

The maxwellite sample was characterised by SEM/EDS. The backscattering image shows a homogeneous phase (Fig. 1). Chemical data is presented in Fig. 2 and shows a simple composition dominated by Fe, As, Na. Minor amounts of Mn, Ti are also observed. The presence of C is due to the carbon coating.

Arsenate vibrations

According to Myneni et al. [14,15] and Nakamoto [16], $(AsO_4)^{3-}$ is a tetrahedral unit, which exhibits four fundamental vibrations: namely the Raman active ν_1 symmetric stretching vibration (A_1) at around 818 cm^{-1}; the Raman active doubly degenerate ν_2 symmetric bending vibration (E) at 350 cm^{-1}, the infrared and Raman active triply degenerate ν_3 antisymmetric stretching vibration (F_2) at 786 cm^{-1}, and the infrared and Raman active triply degenerate ν_4 bending vibration (F_2) at 405 cm^{-1}. Protonation, metal complexation, and/or adsorption on a mineral surface will cause the change in $(AsO_4)^{3-}$ symmetry from T_d to lower symmetries, such as C_{3v}, C_{2v} or even C_1. This loss of degeneracy causes splitting of degenerate vibrations of $(AsO_4)^{3-}$ and the shifting of the As-OH stretching vibrations to different wavenumbers.

Such chemical interactions reduce $(AsO_4)^{3-}$ tetrahedral symmetry, as mentioned above, to either C_{3v}/C_3 (corner-sharing), C_{2v}/C_2 (edge-sharing, bidentate binuclear), or C_1/C_s (corner-sharing,

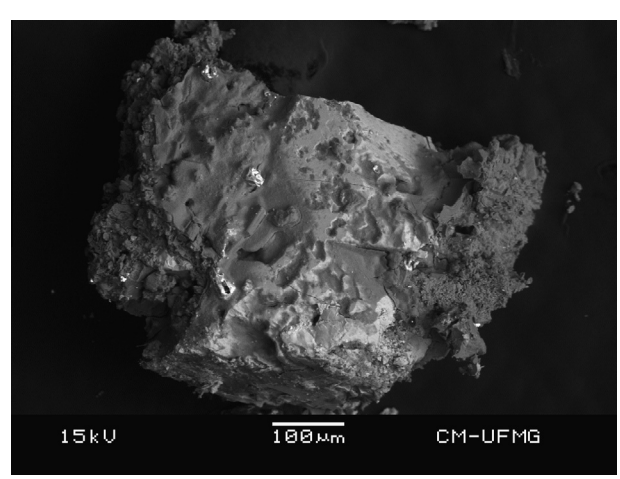

Fig. 1. SEM image of the maxwellite mineral sample.

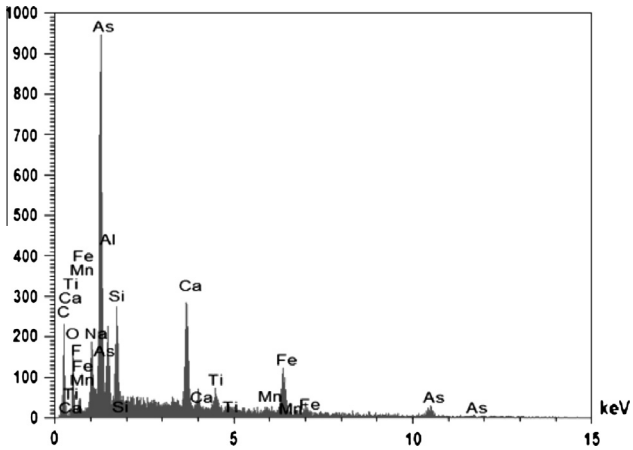

Fig. 2. EDS spectrum of maxwellite.

edge-sharing, bidentate binuclear, multidentate) [14,15]. In association with $(AsO_4)^{3-}$ symmetry and coordination changes, the A_1 band may shift to different wavenumbers and the doubly degenerate E and triply degenerate F modes may give rise to several new A_1, B_1, and/or E vibrations [14,15]. In the absence of symmetry deviations, $(AsO_3OH)^{2-}$ in C_{3v} symmetry exhibit the ν_s As-OH and ν_{as} and ν_s $(AsO_3OH)^{2-}$ vibrations together with corresponding the δ As-OH in-plane bending vibration, δ As-OH out-of-plane bending vibration, ν_s $(AsO_3OH)^{2-}$ stretching vibration and δ_{as} $(AsO_3OH)^{2-}$ bending vibration [17–19]. Keller [17] observed the following infrared bands in $Na_2(AsO_3OH)\cdot 7H_2O$ 450 and assigned bands at 360 cm^{-1} to δ_{as} (ν_4) $(AsO_3OH)^{2-}$ bend (E), 580 cm^{-1} to the δ As-OH out-of-plane bend, 715 cm^{-1} to the ν As-OH stretch (A_1), 830 cm^{-1} to the ν_{as} $(AsO_3OH)^{2-}$ stretch (E), and 1165 cm^{-1} to the δ As-OH in plane bend. In the Raman spectrum of $Na_2(AsO_3OH)\cdot 7H_2O$, Vansant and Veken [18] attributed Raman bands to the following vibrations 55, 94, 116 and 155 cm^{-1} to lattice modes, 210 cm^{-1} to ν (OH...O) stretch, 315 cm^{-1} to $(AsO_3OH)^{2-}$ rocking, 338 cm^{-1} to the δ_s $(AsO_3)^{2-}$ bend, 381 cm^{-1} to the δ_{as} $(AsO_3OH)^{2-}$ bend, 737 cm^{-1} to the ν_s As-OH stretch (A_1), 866 cm^{-1} to the ν_{as} $(AsO_3OH)^{2-}$ stretch (E).

Raman spectroscopy

The Raman spectra of maxwellite and tilasite over the 100–4000 cm^{-1} spectral range are displayed in Fig. 3a and b respectively. These spectra show the position and relative intensities of the Raman bands. It is obvious that there are large parts of the spectra where no intensity is observed and so the spectra are subdivided into sections based upon the type of molecular vibration being studied.

The infrared spectra of these two minerals are given in the supplementary information. The infrared spectra of maxwellite and tilasite over the 500–4000 cm^{-1} spectral range are reported in Fig. S1a and b respectively. These spectra show the positions of the infrared peaks and the relative intensities of these peaks. The infrared spectra of maxwellite over the 650–1200 cm^{-1} spectral range and of tilasite over the 650–950 cm^{-1} spectral range are reported in Fig. S2a and b respectively. These spectra are plotted over different spectral ranges because in the first spectrum (maxwellite), there are a series of peaks which are not observed in the spectrum of tilasite. These additional peaks are attributable to phosphate vibrations, showing that there is some isomorphous substitution of arsenate by phosphate in the structure of maxwellite.

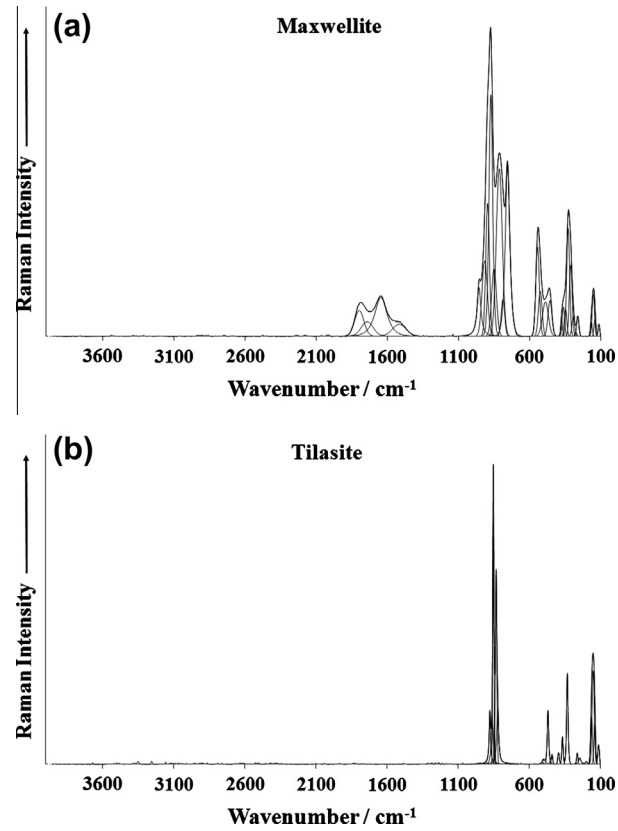

Fig. 3. (a) Raman spectrum of maxwellite in the 4000–100 cm^{-1} region (b) (a) Raman spectrum of tilasite in the 4000–100 cm^{-1} region.

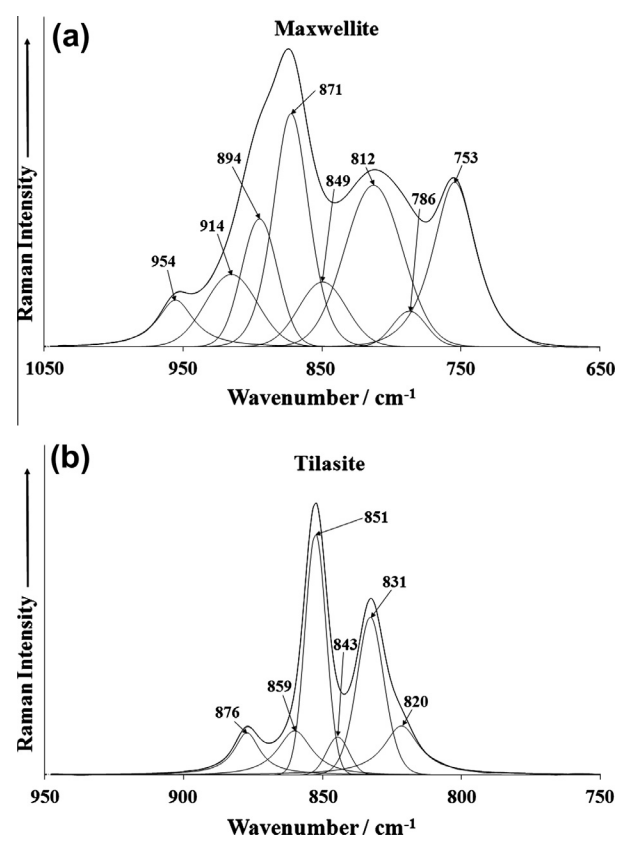

Fig. 4. (a) Raman spectrum of maxwellite in the 650–1050 cm^{-1} region (b) Raman spectrum of tilasite in the 750–950 cm^{-1} region.

The Raman spectrum of maxwellite over the 650–1050 cm^{-1} spectral range is provided in Fig. 4a. Whereas the Raman spectrum of tilasite over the 750–950 cm^{-1} spectral range is illustrated in Fig. 4b. The Raman spectrum of maxwellite in this part of the spectrum appears more complex than that for tilasite. The Raman spectrum of tilasite is characterised by sharp bands. The two highest intensity bands are observed at 851 and 831 cm^{-1} and are assigned to the Raman active ν_1 symmetric stretching vibration (A_1) and the Raman active triply degenerate ν_3 antisymmetric stretching vibration (F_2). A shoulder band at 820 cm^{-1} is probably also due to this vibrational mode. In mineral chemistry the size of F^- ion is almost identical t that of the OH^- ion. Hence, the F^- anion may simply replace the OH^- anion. In the absence of symmetry deviations, $(AsO_3OH)^{2-}$ in C_{3v} symmetry exhibit the ν_s As-OH and ν_{as} and ν_s $(AsO_3OH)^{2-}$ vibrations together with corresponding the δ As-OH in-plane bending vibration, δ As-OH out-of-plane bending vibration, ν_s $(AsO_3OH)^{2-}$ stretching vibration and δ_{as} $(AsO_3OH)^{2-}$ bending vibration [17–19]. Thus, it is proposed that the band at 876 cm^{-1} and the 859 cm^{-1} band is ascribed to the ν_s and ν_{as} $(AsO_3F)^{2-}$ vibrations. The assignment of the Raman bands for maxwellite in this spectral region is complicated by the presence of phosphate in the structure as is evidenced by the infrared spectrum (Fig. S2a). The Raman band of maxwellite at 871 cm^{-1} is assigned to the ν_1 symmetric stretching vibration and the Raman band at 812 cm^{-1} is assigned to the ν_3 antisymmetric stretching vibration. It is thought that the Raman bands at 894 and 849 cm^{-1} are due to the to the ν_s and ν_{as} $(AsO_3F)^{2-}$ vibrations. The Raman bands at 914 and 954 cm^{-1} are due to phosphate vibrations.

In the Raman spectrum of maxwellite downloaded from the RRUFF data base, two intense sharp peaks are observed at 866 and 794 cm^{-1} and are assigned to the symmetric and antisymmetric stretching vibrations of the AsO_4^{3-} units. Two broad bands are found at 630 and 650 cm^{-1}. It is not known to what these bands may be assigned. In the Raman spectrum of tilasite downloaded from the RRUFF data base, a very intense sharp band at 850 cm^{-1} is observed with two shoulder bands of much lower intensity at 828 and 874 cm^{-1}. The position of the Raman bands for tilasite from the RRUFF data base is in good agreement with the Raman spectrum of tilasite reported in this work. Some variation in intensity is found between the two Raman spectra of tilasite but this may be simply due to orientation effects.

In the infrared spectrum of maxwellite and tilasite, the infrared bands overlap but nevertheless band component analysis does enable the component bands to be resolved. The infrared spectrum of maxwellite over the 650–1200 cm^{-1} spectral range is shown in Fig. S2a. The infrared spectrum of tilasite over the 650–1200 cm^{-1} spectral range is shown in Fig. S2b. The broad infrared spectral profile of maxwellite between 650 and 950 cm^{-1} are attributed to AsO_4^{3-} stretching vibrations. The broad infrared profile between 950 and 1150 cm^{-1} are due to phosphate bands. Band separation is slightly better for tilasite. The infrared bands between 650 and 950 cm^{-1} are attributed to arsenate stretching vibrations.

The complexity of the Raman spectra of maxwellite is reflected in the 400–600 cm^{-1} spectral region (Fig. 5a). Here we observed four peaks at 455, 487, 523 and 542 cm^{-1}. These bands are broad and reflect the complexity of the phosphate units in the maxwellite structure. In some ways the RRUFF spectrum resembles this spectrum (Fig. 5a). The RRUFF spectrum shows a band at 526 cm^{-1} with another band at around 489 cm^{-1}. This latter band is assigned to the Raman active triply degenerate ν_4 bending vibration (F_2).

The Raman spectrum of tilasite in the 300–550 cm^{-1} spectral region is shown in Fig. 5b. The intense Raman band of tilasite at 467 cm^{-1} is assigned to the Raman active triply degenerate ν_4 bending vibration (F_2). The other low intensity Raman bands at 438, 450, 494 and 501 cm^{-1} of tilasite are probably due to this vibration and simply served to show there is a reduction of symmetry of the arsenate anion in the tilasite structure. The intense Raman band at 331 cm^{-1} for tilasite is assigned to the Raman active doubly degenerate ν_2 symmetric bending vibration (E). The two other Raman bands at 365 and 393 cm^{-1} are also attributed to this vibration. The Raman spectrum of tilasite downloaded from the RRUFF data base shows Raman bands at 327, 360, 380, 463 and 501 cm^{-1}. The position of these bands is in reasonable agreement with the position of the bands reported here. As would be expected the position of the Raman bands in this spectral region will be a function of the chemical composition which in turn is a function of the origin of the sample.

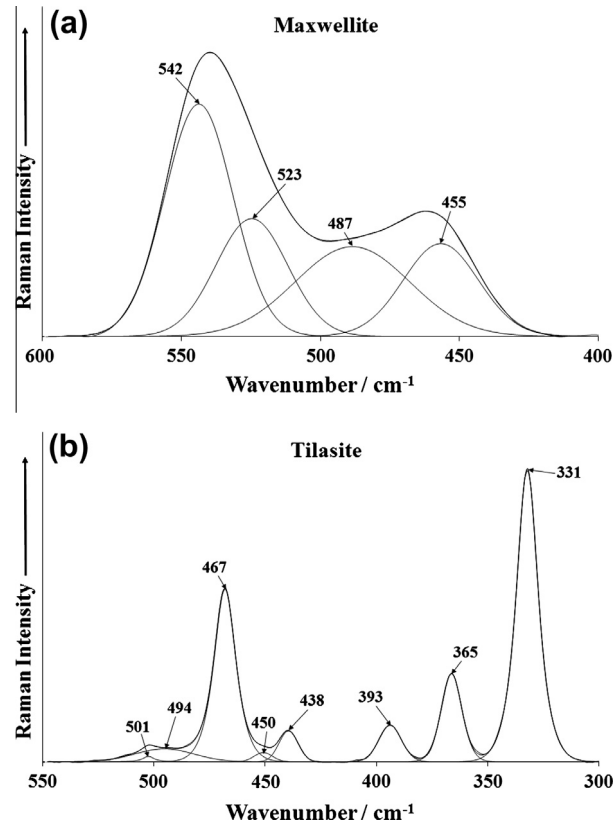

Fig. 5. (a) Raman spectrum of maxwellite in the 400–600 cm^{-1} region (b) Raman spectrum of tilasite in the 300–550 cm^{-1} region.

The Raman spectrum of maxwellite in the 100–400 cm^{-1} spectral region is illustrated in Fig. 6a and the Raman spectrum of tilasite in the 100–300 cm^{-1} spectral region is illustrated in Fig. 6b. Intense Raman bands for maxwellite are observed at 309 and 327 cm^{-1} with shoulder bands at 291, 346, 360 and 373 cm^{-1}. It is thought that these bands are due to metal oxygen stretching vibrations. Other bands for maxwellite at 111, 140, 154 and 164 cm^{-1} are noted and are described as lattice vibrations. The intensity of these lattice bands for tilasite show much greater intensity. Raman bands are noted at 111, 139, 149 and 160 cm^{-1}. The spectrum of maxwellite and tilasite are very similar in this part of the spectrum.

It should be noted that formula of the minerals, maxwellite, tilasite and durangite show the absence of water and OH units. This is also observed by the lack of signal in the Raman spectrum of maxwellite and tilasite (see Fig. 3a and b). It is obvious that no intensity exists in the OH stretching region. In the infrared spectrum of maxwellite no intensity in the OH stretching region was found. However very weak infrared bands for tilasite were observed at 3196 and 3437 cm^{-1} and were assigned to adsorbed water.

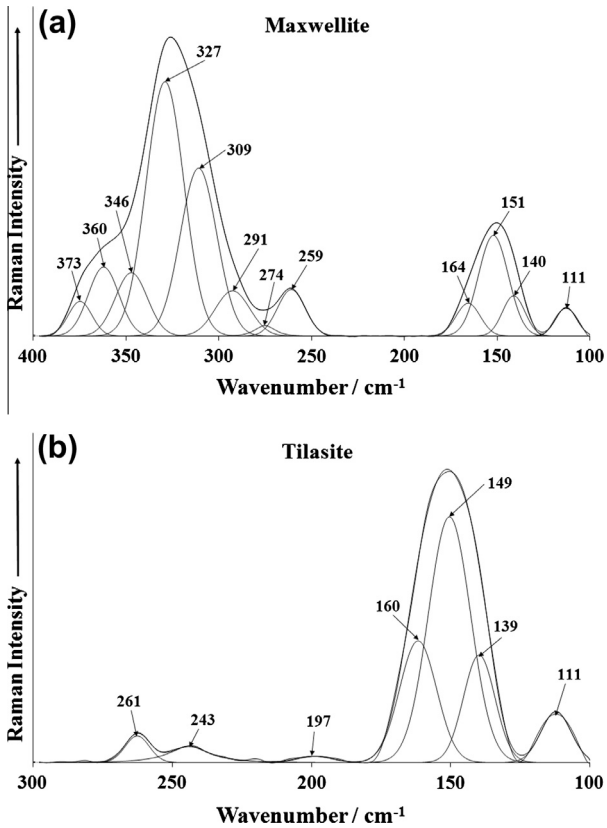

Fig. 6. (a) Raman spectrum of maxwellite in the 100–400 cm^{-1} region (b) Raman spectrum of tilasite in the 100–300 cm^{-1} region.

Conclusions

We have used a combination of scanning electron microscopy with EDX and both Raman and infrared spectroscopy to study the chemistry and molecular structure of the mineral maxwellite $NaFe^{3+}(AsO_4)F$. A comparison is made with the spectroscopy of tilasite $CaMg(AsO_4)F$. SEM identifies a single phase. Chemical analysis shows that maxwellite is composed of Fe, Na and Ca with minor amounts of Mn and Al. The molecular structure of maxwellite and tilasite were analysed by Raman and infrared spectroscopy. Raman bands are assigned to the AsO_4^{3-} stretching and bending vibrations. No bands attributable to water or hydroxyl stretching vibrations were observed.

Appendix A. Supplementary material

Supplementary data associated with this article can be found, in the online version, at http://dx.doi.org/10.1016/j.saa.2013.12.081.

References

[1] E.E. Foord, P.F. Hlava, J.J. Fitzpatrick, R.C. Erd, R.W. Hinton, Neues Jb. Miner. Mh. (1991) 363–384.
[2] F.J. Parker, T.A. Peters, Miner. Rec. 9 (1978) 385–386.
[3] S.A.H. Sjogren, Geol. Foren. i Stockholm Forh. 17 (1895) 291–294.
[4] E.E. Foord, M.R. Oakman, C.H. Maxwell, Can. Miner. 23 (1985) 241–246.
[5] S.I. Lahti, A. Pajunen, Am. Miner. 70 (1985) 849–855.
[6] F. Machatschki, Zeit. fuer Krist. 103 (1941) 221–227.
[7] G.J. Brush, Am. J. (1901) Sc. xi 464–465.
[8] M.A. Cooper, F.C. Hawthorne, Neues Jb. Miner. Mh. (1995) 97–104.
[9] M. Reynaud, P. Barpanda, G. Rousse, J.-N. Chotard, B.C. Melot, N. Recham, J.-M. Tarascon, Solid State Sc. 14 (2012) 15–20.
[10] K.W. Bladh, R.K. Corbett, W.J. McLean, R.B. Laughon, Am. Miner. 57 (1972) 1880–1884.
[11] P. Kokkoros, Naturwissenschaften 25 (1937) 717.
[12] P. Kokkoros, Zeit. fuer Krist. 99 (1938) 39–49.
[13] J.W. Anthony, R.A. bideaux, K.W. Bladh, M.C. Nichols, Silica, Silicates, Mineral data Publishing, Tucson, Arizona, 1995.
[14] S.C.B. Myneni, S.J. Traina, G.A. Waychunas, T.J. Logan, Geochim. Cosmochim. Acta 62 (1998) 3285–3300.
[15] S.C.B. Myneni, S.J. Traina, G.A. Waychunas, T.J. Logan, Geochim. Cosmochim. Acta 62 (1998) 3499–3514.
[16] K. Nakamoto, Infrared and Raman Spectra of Inorganic and Coordination Compounds., Wiley, New York, 1986.
[17] P. Keller, Neues Jb. Miner. Mh. (1971) 491–510.
[18] F.K. Vansant, B.J.V.D. Veken, J. Mol. Struct. 15 (1973) 439–444.
[19] F.K. Vansant, B.J.V.D. Veken, H.O. Desseyn, J. Mol. Struct. (1973) 425–437.